Title: Critical Current for Phase Shift of Dry-Band Discharge on Wet Polluted Insulators

Authors: Takahiko Yamashita*[1], Tomohiro Furusato[1], Ryo Konishi[1], Takafumi Kurokawa[1], and Kohei Yaji[2],

1: Nagasaki University, Nagasaki 852-8521, Japan

2: National Institute of Technology, Kagoshima College, Kirishima City, Kagoshima 899-5193, Japan

*Correspondence author (e-mail address): yamac@nagasaki-u.ac.jp (Takahiko Yamashita)

Abstract: This paper presents experimental results on the influence of the electrolyte on the phase shift of dry-band discharges. Two types of electrolytes (NaCl and $MgCl_2$) were introduced to compare the case of KCl, and a model electrode system including glass-filter electrodes wetted with an aqueous solution of the electrolyte was employed to simulate a dry band. The spectral emission intensity originated from the electrolyte depended on the electrolyte and was strongly affected by the peak value of the current during the continuous dry-band discharge. Finaly, the critical current was found to be approximately 3 mA irrespective of the electrolytes examined.

1. Introduction

Surface discharge on wet polluted insulators has been a serious problem because the flashover voltage of wet polluted insulators becomes extremely low. Recently, this has attracted attention from the point of view of the deterioration of polymer insulators (e. g. [1]-[2]). The deterioration is caused by the discharge across the polymeric material. In order to discuss such as this deterioration, characteristics of the surface discharge should be expressed precisely. However, to date, little research has been carried out to understand such surface discharge characteristics [3].

Regarding the surface discharge on wet polluted insulators, the mechanism of this surface discharge is explained as follows [4]. Surface discharge occurs when a leakage current forms a dry band by Joule heating. When this dry band is formed and full voltage is applied across the dry band, local discharge occurs at the dry band. Then, in the presence of a wet polluted surface a local discharge propagates, and surface flashover will occur when the local discharge bridges the terminals. The surface flashover voltage for a given insulator is generally expressed as a function of the surface resistance which depends on the deposit density of electrolytic pollutants. The electrolytic pollutants may affect the discharge behavior. Therefore, it is important to understand the influences of these various electrolytes on the discharge characteristics. The electrode fall voltage of the local discharge is typically several hundred volts [5]-[6], which is much higher than that of the free arc between metal electrodes. The current density increases with the air pressure [7]. Compared with discharge in the air the propagation velocity of the surface discharge is lower than that of streamers and is in the same order of that of a leader [8]-[9].

The interaction between plasma and liquid however, has attracted significant attention in the field of electrochemistry. In relation to waste-water treatment, etc., discharges on water has been well investigated. Research on discharges on water has been reviewed by Bruggeman et al. [10]-[11]. Mezei and Cserfalvi [12] have reviewed research on electrolyte cathode atmospheric glow discharge in relation to the measure of water containing toxic heavy metals. However, interactions between discharge plasma and solutions including electrolytes, organic materials, etc. have not been fully understood.

In both fields of research, understanding the mechanism of the interaction at the surface of the solution is important. This paper describes the influence of the electrolyte on the phase shift of the dry-band discharge. Two more kinds of electrolytes (NaCl and $MgCl_2$) have been introduced to compare with potassium chloride (KCl) which was used in the previous study [13], and a model electrode system has been employed to simulate the dry band. The influence of the electrolytes on the critical current was examined. As for the discharge current, the

authors mainly focused on the continuous discharge in this paper because the pulsative current of the intermittent dry-band discharge was found to be an apparent current.
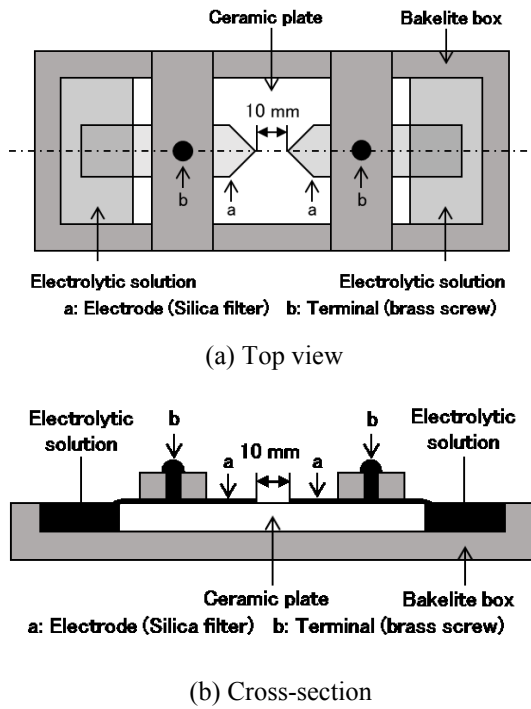

(a) Top view

(b) Cross-section

Figure 1. Electrode arrangement.

2. Experimental Setup and Procedure

Figure 1 shows a model electrode system which is the same as in the previous study [13]. Figure 1a and 1b show the top view of the experimental set-up and the cross-section at the center (dashed line), respectively. The electrode system simulates a dry band on an insulator surface. The electrode was made of silica filter and was wetted with an aqueous solution. In this study, sodium chloride (NaCl) and magnesium chloride ($MgCl_2$) were used to compare with the previously investigated potassium chloride (KCl). The aqueous solution was stored in trenches made at both ends of the Bakelite box, as shown in Figure 1b. The resistivity of the aqueous solution was measured with a conductivity meter (DKK Corporation, AOL-40) and was set to 20 Ωcm at 20 degrees Celsius. The resistivity was set accordingly by taking various tracking and erosion tests from our previous study [5] into consideration. Electrodes were placed on a ceramic plate so that their tips were facing each other and had a gap of 10 mm. The electrodes were held with brass screws, which were also used as terminals to connect the

cables. The electrodes were connected to a high voltage transformer (Tokyo Transformer Co., Ltd., T-G-50) with a capacity of 5 kVA. The frequency of the ac power source was 60 Hz.

Figure 2 shows a schematic diagram of the experimental setup and the measuring system which are almost the same as in the previous study [13]. A resistor R_1 used to control the discharge current was connected in series to the model electrodes system. The resistance (R_1) was varied in the range between 2 and 7 MΩ. Ac high voltage was applied to the electrodes to initiate a dry-band discharge. The peak value of the applied voltage was approximately 22 kV and was larger than the discharge onset voltage of the gap. The applied voltage and the values of the series resisters were selected so that stable dry-band discharge took place.
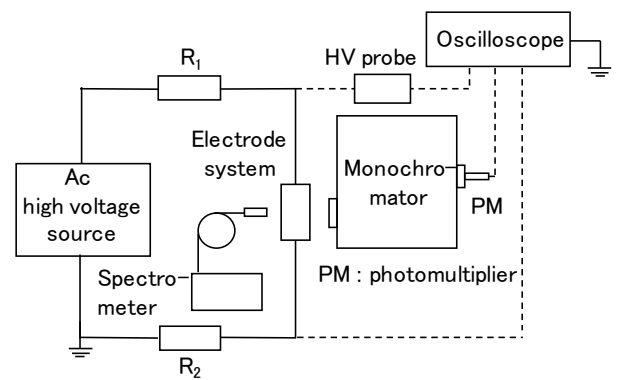

Figure 2. Schematic diagram of the experimental setup and measuring system.

The voltage between the terminals was measured with a high voltage probe (Iwatsu HV-P60) and a digital oscilloscope (Tektronix Inc., DPO-4104B-L). The current through the gap was obtained from the voltage drop of a current measuring resistor R_2 whose resistance was 47 Ω, and the waveform was observed with the digital oscilloscope.

The spectrum distribution from the discharge was measured with a spectrometer (BWTEK Inc., Glacier X). The temporal variations of the emission spectra, which originated from nitrogen molecules and the electrolyte, were measured with a monochromator (Ritsu Oyo Kougaku Co., Ltd., MC-25NP) and the digital oscilloscope. The resolution of the monochromator was determined by the width of the output slit and was 2.9 nm/mm. The apertures of the input and output slits were set to 2 mm in order to observe double lines simultaneously. The distance between the discharge and the input slit was set to 200 mm. The output light from the monochromator was converted to an electric signal using a photomultiplier system (Hamamatsu Photonics, H10720-01) and was measured with the digital oscilloscope. Images of the discharge were also recorded using a digital camera (Nikon, D610). The rotational temperature was decided from the spectral profile of the N_2 second positive system band (N_2 2PB), details regarding this

3. Experimental Results and Discussion
3.1 Typical discharge patterns

The voltage and current waveforms and the variation of light emission in the cases of aqueous solutions of sodium chloride (NaCl) and magnesium chloride ($MgCl_2$) were similar to that of potassium chloride (KCl) [13]. Two types of dry-band discharges, the continuous and intermittent discharges, were also observed in the cases of the solutions of NaCl and $MgCl_2$. The continuous discharge is characterized by the continuous current and light emission as shown in Figure 3. On the other hand, the intermittent discharge is characterized by the pulsative current and intermittent light emission as shown in Figure 4. A continuous discharge was observed at a relatively low value of series resistance, while the intermittent discharge was observed at a relatively high value.

(a) Voltage waveform

(b) Current waveform
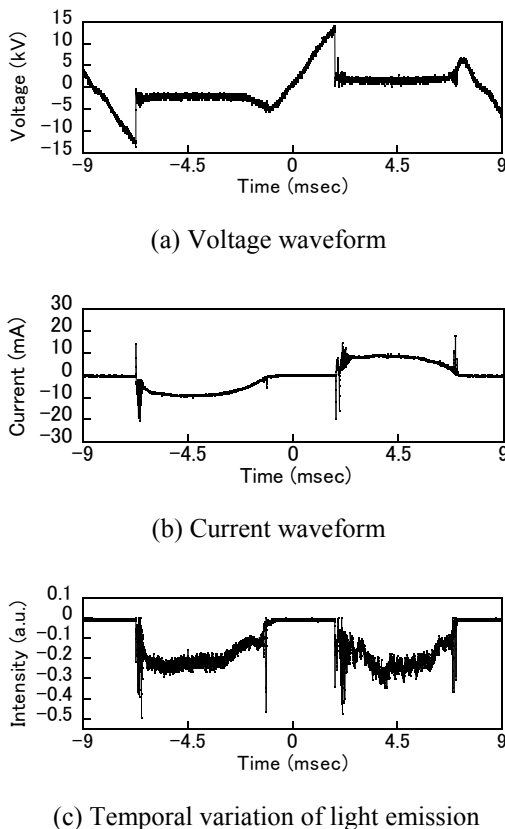

(c) Temporal variation of light emission

Figure 3. An example of the results of simultaneous measurement of voltage and current waveforms, and temporal variation of light emission in the case of the continuous dry-band discharge (NaCl aq.: R_1=2 (MΩ)).

are outlined in [13].

(a) Voltage waveform

(b) Current waveform
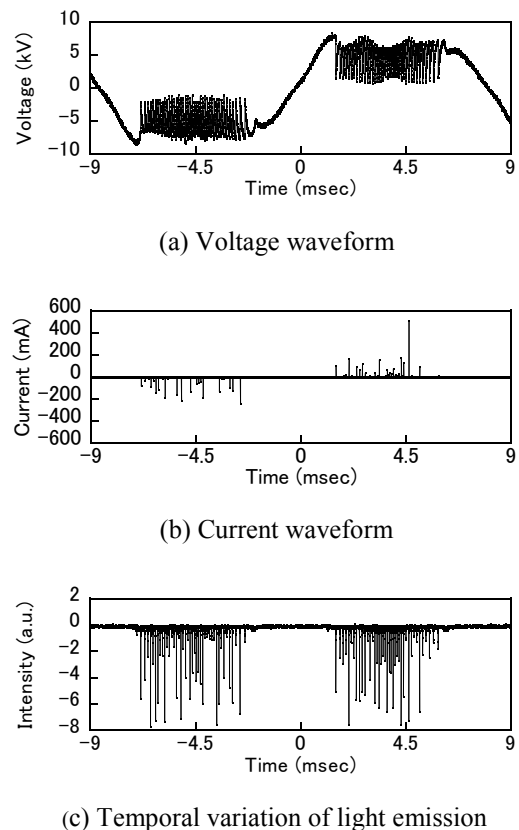

(c) Temporal variation of light emission

Figure 4. An example of the results of simultaneous measurement of voltage and current waveforms, and temporal variation of light emission for intermittent dry-band discharge (NaCl aq.: R_1=7 (MΩ)).

3.2 Emission spectrum and gas temperature

Figure 5 shows the spectral distributions in the case of continuous dry-band discharge when R_1=2 (MΩ). The spectra originated from the electrolytes (Na: 589.0, 589.6 nm, Mg: around 309, 383, 517 nm), especially Na, was significantly stronger. On the other hand, the intensity of N_2 for $MgCl_2$ was slightly higher than that of NaCl.

Figure 6 shows the photographs of the dry-band discharges and illustrations of the outline images of the area of light emission originated from the electrolyte. These photographs were taken with a digital camera and with 1/250 s shutter speed. They were taken when the value of the series resistance was 2 MΩ. In the cases of NaCl, the light emission originated from the electrolyte can be seen entire the discharge channel. On the other hand, the light emission is weak and is seen partially in the case of $MgCl_2$.

Figure 7 shows the spectral distributions in the case of the intermittent dry-band discharge when R_1=7 (MΩ). The spectrum intensity of N_2 was of the same order irrespective of
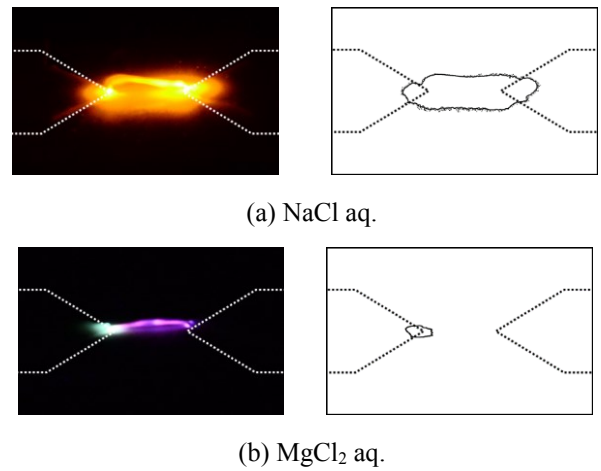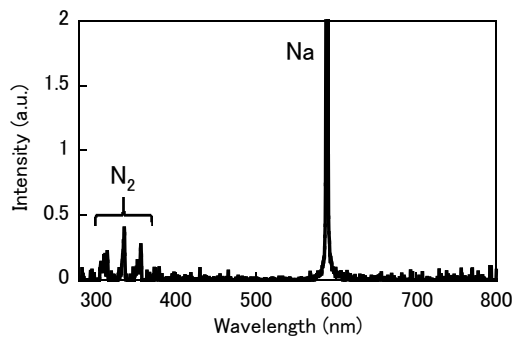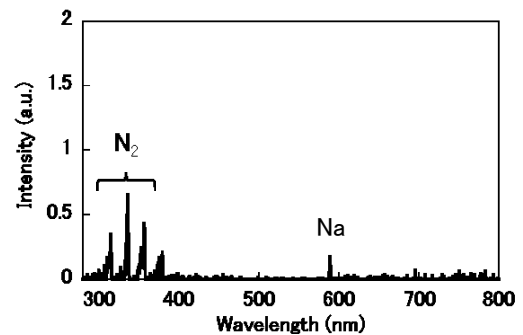

(a) NaCl aq.

(b) $MgCl_2$ aq.

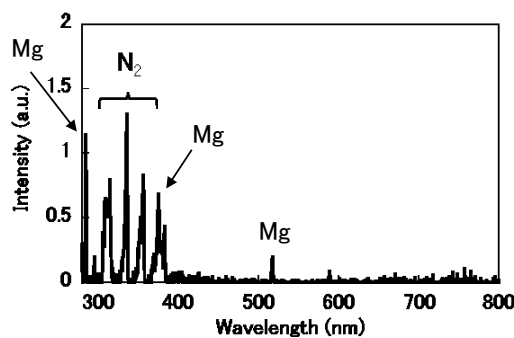Figure 6. Photographs of the dry-band discharges.

the electrolyte. The spectral intensity originating from Na was comparable with that of N_2, as shown in Figure 7a. However, the spectral intensity originating from Mg was much smaller than that of N_2, sometimes it was not observed, as shown in Figure 7b.
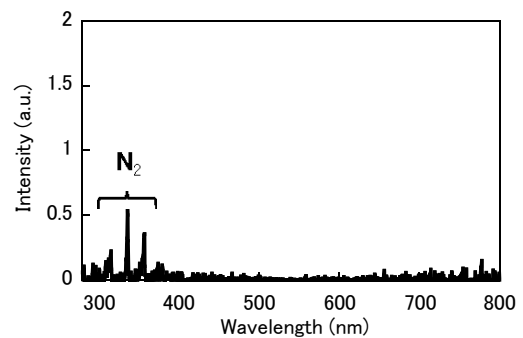

(a) NaCl aq. (R_1=2 (MΩ))

(b) $MgCl_2$ aq. (R_1=2 (MΩ))

Figure 5. Spectral distributions from the continuous dry-band discharges.

(a) NaCl aq. (R_1=7 (MΩ))

(b) $MgCl_2$ aq. (R_1=7 (MΩ))

Figure 7. Spectral intensity distributions from the intermittent dry-band discharges.

Table 1 shows the estimated gas temperatures of the intermittent and continuous dry-band discharges for the solutions of KCl [13], NaCl and MgCl$_2$. The gas temperature was obtained from the rotational temperature by matching the measured profile of the spectral distribution of N$_2$ 2PB with the theoretical profile. The gas temperature was approximately 6000-6200 K for the continuous dry-band discharge. On the other hand, it was 1700-1800 K for the intermittent dry-band discharge. Thus, the gas temperature of the continuous dry-band discharge was somewhat higher than that of the intermittent dry-band discharge.

Table 1. Estimated gas temperature.

| Electrolytic solution	Estimated gas temperature	
	Intermittent	Continuous
KCl aq.	1800 K	6000 K
NaCl aq.	1700 K	6000 K
MgCl$_2$ aq.	1700 K	6200 K

3.3 Temporal occupancy ratios of continuous and intermittent discharges

Two types of dry-band discharges were observed in this experiment, one using a low resistance (2 MΩ) and the other a higher resistance (7 MΩ). The types were determined from the voltage, current waveforms, and the temporal variations of light emission. In this section, intermediate range values of series resistance were chosen between 2 to 7 MΩ.

The observed results showed that both types of discharges alternately appeared in a half cycle of the applied voltage but did not appear at the same time. Figure 8 shows the variation of the temporal-occupancy ratio of each discharge type as a function of the value of the series resistance. The temporal-occupancy ratio was obtained from the duration of each discharge type divided by the total discharge period. The temporal-occupancy ratio of continuous discharge decreased with the value of the series resistance. On the other hand, the temporal-occupancy ratio of intermittent discharge increased with the value of the series resistance. The temporal-occupancy
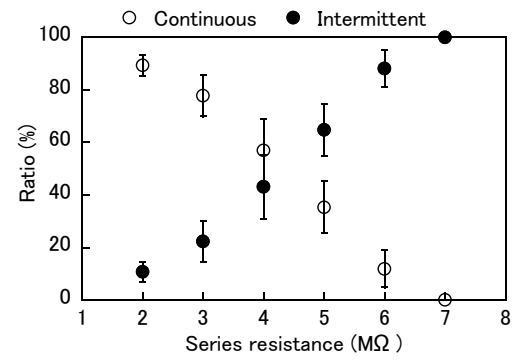
(a) NaCl aq.
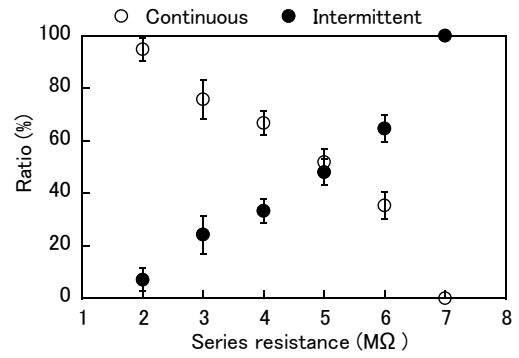
(b) MgCl$_2$ aq.

Figure 8. Variation of the ratios of the duration of the continuous and intermittent discharges as a function of the value of the series resistance.

ratios cross at a series resistance of 4-5 MΩ.

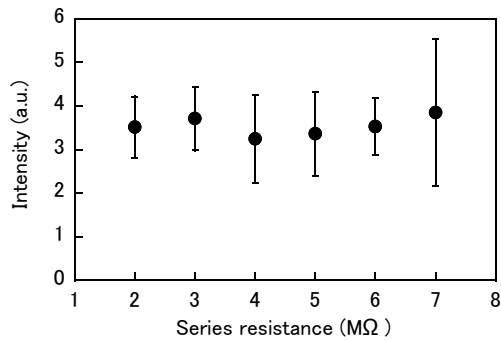### 3.4 Spectral emission intensity and discharge current
3.4.1 Spectral emission intensity

Figure 9 shows the relation between the peak value of the spectral emission of N$_2$ 2PB during the intermittent dry-band discharge and the value of the series resistance. The spectrum intensity of N$_2$ 2PB was measured at 336.6 nm with a monochromator. In both electrolytes, the peak values of the spectral emission of N$_2$ 2PB were independent of the value of the series resistance. It is similar to the case of KCl [13]. Therefore, the emission intensity of N$_2$ 2PB does not depend on the value of the series resistance and the electrolyte.

The intensity of the spectral emission originating from the electrolyte was strong in the period of the continuous dry-band discharge. The relation between the peak value of the spectral
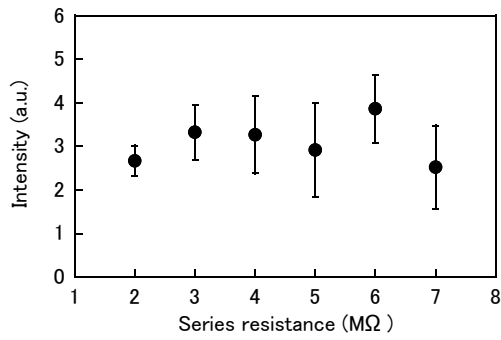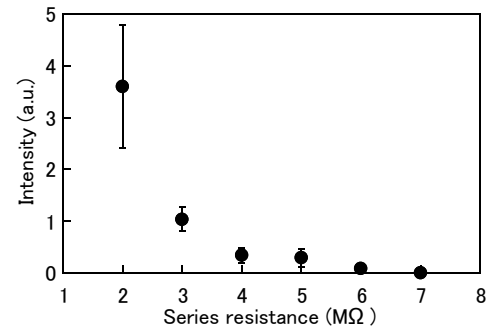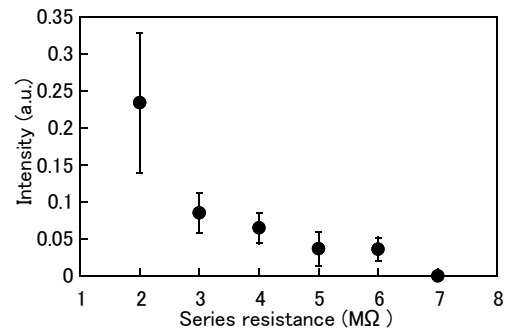
(a) NaCl aq.

(b) MgCl₂ aq.

Figure 9. The relation between the spectral emission intensity originating from nitrogen molecules (366.6 nm) and the value of the series resistance.
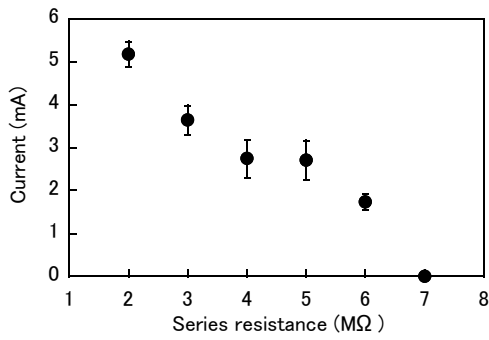

(a) NaCl aq.

(b) MgCl₂ aq.

Figure 10. The relation between the spectral emission intensity originating from the electrolyte and the value of the series resistance.

emission originating from the electrolyte during the continuous dry-band discharge and the value of the series resistance is shown in Figure 10. The spectral intensities originating from the electrolyte were measured at 589.3 nm for Na and 518.1 nm for Mg, respectively with a monochromator. The peak value of the spectral emission originating from the electrolyte decreased as the series resistance decreased. This tendency was similar to that of KCl [13] indicating it was invariant to the electrolytes tested. However, the peak value of the spectral emission did vary between electrolytes.

The light emission originating from the electrolyte was affected by the type of electrolyte as can be seen in Figures 5, 6 and 10. The strong spectral emission originating from the electrolyte during the continuous dry-band discharge indicates the sputtering of electrolytic atoms caused by high energy species such as nitrogen molecule ions [10], [14]-[15]. The spectral emission intensity is presumed to be affected by the rates of sputtering and/or excitation in the gas phase plasma.

However, this could not be confirmed. This dependence of the spectral emission originating from the electrolyte on the electrolyte needs to be investigated in the future in more detail.
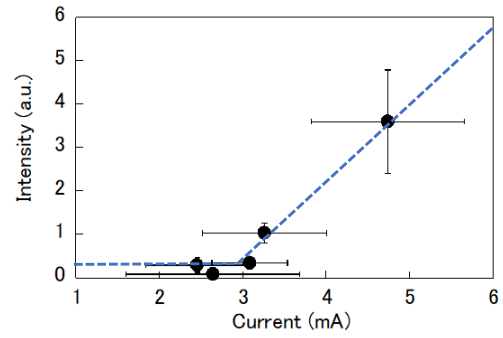
3.4.2 Discharge current

Figure 11 shows the relation between the peak value of the current during continuous discharge and the series resistance. The peak value of the current during the continuous discharge decreased with an increase in the value of the series resistance, except for the case of 7 MΩ. When R_1=7 (MΩ), almost no continuous discharge was observed, irrespective of the electrolyte.
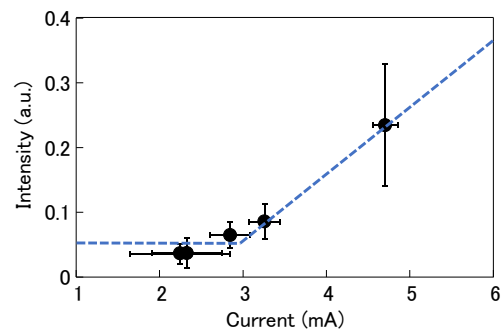
(a) NaCl aq.
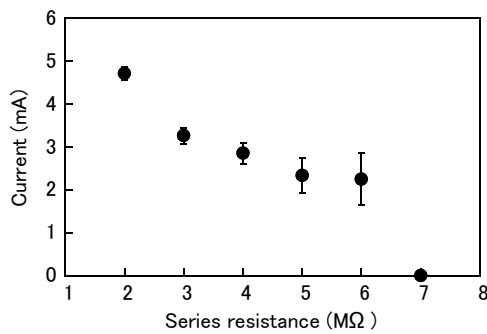
(b) MgCl₂ aq.

Figure 11. The relation between the peak value of the current during continuous discharge and the value of the series resistance.

(a) NaCl aq.

(b) MgCl₂ aq.

Figure 12. The relation between the peak values of the spectral emission intensity originating from the electrolyte and the current during continuous discharge.

3.5 Phase shift of dry-band discharge with regard to discharge current

The relation between the peak value of spectral emission originating from the electrolyte and the peak value of the current during continuous dry-band discharge was obtained from Figures 10 and 11 and is shown in Figure 12. The peak value of spectral emission increased with the peak value of the current and was found to be significantly affected by the current when the value was larger than 3 mA. This was similar to the case of KCl [13]. Therefore, the critical current of the phase shift of the dry-band discharge was found to be around 3 mA irrespective of the electrolyte among those tested.

4. Conclusions

In this paper, the influence of the electrolyte on the phase shift of the dry-band discharge was examined. A model electrode that simulated the dry-band was employed. The influence was examined for the electrolytic solutions of NaCl and MgCl₂ and was compared with the case of KCl. The phase shift of the dry-band discharge was discussed with regard to critical current, spectral emission intensity originating from the electrolyte, etc. The following results were obtained.

1) For each of the electrolytes examined, the continuous and intermittent discharges were observed. The continuous dry-band discharge was observed for a relatively low value of series resistance, and the gas temperature was approximately 6000-6200 K. On the other hand, the intermittent dry-band discharge was observed for a relatively high value of series resistance and the gas temperature of was around 1700-1800 K. The gas temperature was independent of the electrolyte among KCl,

NaCl and MgCl$_2$.

2) The intensity of spectral emission originating from the electrolyte was stronger during continuous discharge compared with the intermittent discharge. The intensity varied significantly with the type of electrolyte. On the other hand, the spectral emission of nitrogen molecules was dominant during the intermittent discharge. The intensity of spectral emission of molecular nitrogen was independent of the series resistance and the electrolyte.

3) The mode of the dry-band discharge varied with the current. The critical current of the phase shift of the dry-band discharge was about 2-3 mA irrespective of the electrolyte. The influence of the electrolytes on the critical current was small.

Acknowledgments

References

[1] V. M. Moreno and R. S. Gorur, Effect of Long-term Corona on Non-ceramic Outdoor Insulator Housing Material, IEEE Trans. Dielect. Electr. Insul., 8 (2001) 117-128.

[2] I. J. S. Lopes, S. H. Shesha, H. Jayaram and E. A. Cherney, A Study of Partial Discharges from Water Droplets on a Silicone Rubber Insulating Surface", IEEE Trans. Dielect. Electr. Insul., 8 (2001) 262-268.

[3] N. Yoshimura, M. Nishida, and F. Noto, Light Emission from Tracking Discharges on Organic Insulation, IEEE Trans. on Electr. Insul., EI-19 (1984) 149-155.

[4] B. F. Hampton, Flashover Mechanism of Polluted Insulation, Proc. IEE, 111 (1961) 985-990.

[5] T. Yamashita, H. Matsuo, H. Fujiyama and T. Oshige, Electrode-Fall of Local Discharge on an Electrolytic Surface, IEEE Trans. Electr. Insul., 23 (1988) 979-986.

[6] P. Bruggeman, E. Ribežl, A. Maslani, J. Degroote, A. Malesevic, R. Rego, J. Vierendeels and C. Leys, Characteristics of Atmospheric Pressure Air Discharges with a Liquid Cathode and a Metal Anode, Plasma Source Sci. Technol., 17 (2008) 025012(11pp).

[7] T. Yamashita, H. Matsuo, Y. Okuno and T. Oshige, Current Density at the Local Discharge Tip on an Electrolytic Surface, IEEE Trans. Electr. Insul., 25 (1990) 1104-1110.

[8] T. Yamashita, H. Matsuo, H. Fujiyama and T. Oshige, Relationship between Photo-Emission and Propagation Velocity of Local Discharge on Electrolytic Surfaces, IEEE Trans. Electr. Insul., EI-22 (1987) 811-817.

[9] H. Matsuo, T. Fujishima, O. Takenouchi and T. Yamashita, Propagation Velocity and Photoemission Intensity of a Local Discharge on an Electrolytic Surface, IEEE Trans. Dielect. Electr. Insul., 3 (1996) 444-449.

[10] P. J. Bruggeman, M. J. Kurshner, B. R. Locke, J. G. E. Gardeniers, W. G. Graham, D. B. Graves, H. C. H. M. Hofman-Caris, D. Maric, J. P. Reid, E. Ceriani, D. Fernandez Rivas, J. E. Foster, S. C. Garrick, Y. Gorbanev, S. Hamaguchi, F. Iza, H. Jablonowski, E. Klimova, J. Kolb, F. Krema, P. Lukes, Z. Machala, I. Marinov, D. Mariotti, S. Mededovic Thagard, D. Minakata, E. C. Nevts, J. Pawlat, Z. Lj Petrovic, R. Pflieger, S. Reuter, D. C. Schram, S. Schröter, M. Shiraiwa, B. Tarabová, P. A. Tsai, J. R. R. Verlet, T. von Woedike, K. R. Wilson, K. Yasui and G. Zvereva, Plasma-Liquid Interactions: A Review and Roadmap, Plasma Source Sci. Technol., 25 (2016) 053002(59pp).

[11] P. Bruggeman and C. Leys, Non-thermal Plasmas in and in Contact with Liquids", J. Phys. D: Appl. Phys. 42 (2009) 053001 (28pp).

[12] P. Mezei and T. Cserfalvi, Electrolyte Cathode Atmospheric Glow Discharges for Direct Solution Analysis, Applied Spectroscopy Reviews, 42 (2007) 573-604.

[13] T. Yamashita, R. Ishimoto and T. Furusato, Influence of Series Resistance on Dry-Band Discharge Characteristics on Wet Polluted Insulators, IEEE Trans. Dielect. Electr. Insul., 25 (2018) 154-161.

[14] Y. Minagawa, N. Shirai, S. Uchida and F. Tochikubo, Analysis of Effect of Ion Irradiation to Liquid Surface on Water Molecule Kinetics by Classical Molecular Dynamics Simulation, Japanese J. Appl. Phys., 53 (2014) 010210 (7 pages).

[15] P. Mezei, T. Cserfalvi and M. L. Nossy, Pressure Dependence of the Atmospheric Electrolyte Cathode Glow Discharge Spectrum, Journal of Analytical Atomic Spectrometry, 12 (1997) 1203–1208.